Glioblastoma endothelium drives bevacizumab-induced infiltrative growth *via* modulation of PLXDC1

Maria Laura Falchetti[1]*, Quintino Giorgio D'Alessandris[2]*, Simone Pacioni[2]*, Mariachiara Buccarelli[3], Liliana Morgante[4], Stefano Giannetti[4], Valentina Lulli[3], Maurizio Martini[5], Luigi Maria Larocca[5], Eliza Vakana[6], Louis Stancato[6], Lucia Ricci-Vitiani[3] and Roberto Pallini [ORCID][2]

[1]CNR-Institute of Cell Biology and Neurobiology (IBCN), Rome, Italy

[2]Institute of Neurosurgery, Fondazione Policlinico Universitario A. Gemelli IRCCS - Università Cattolica del Sacro Cuore, Rome, Italy

[3]Department of Oncology and Molecular Medicine, Istituto Superiore di Sanità, Rome, Italy

[4]Institute of Anatomy and Cell Biology, Università Cattolica del Sacro Cuore, Rome, Italy

[5]Pathology, Fondazione Policlinico Universitario A. Gemelli IRCCS - Università Cattolica del Sacro Cuore, Rome, Italy

[6]Discovery Research, Eli Lilly and Company, Indianapolis, IN

Bevacizumab, a VEGF-targeting monoclonal antibody, may trigger an infiltrative growth pattern in glioblastoma. We investigated this pattern using both a human specimen and rat models. In the human specimen, a substantial fraction of infiltrating tumor cells were located along perivascular spaces in close relationship with endothelial cells. Brain xenografts of U87MG cells treated with bevacizumab were smaller than controls ($p = 0.0055$; Student t-test), however, bands of tumor cells spread through the brain farther than controls ($p < 0.001$; Student t-test). Infiltrating tumor Cells exhibited tropism for vascular structures and propensity to form tubules and niches with endothelial cells. Molecularly, bevacizumab triggered an epithelial to mesenchymal transition with over-expression of the receptor Plexin Domain Containing 1 (PLXDC1). These results were validated using brain xenografts of patient-derived glioma stem-like cells. Enforced expression of PLXDC1 in U87MG cells promoted brain infiltration along perivascular spaces. Importantly, PLXDC1 inhibition prevented perivascular infiltration and significantly increased the survival of bevacizumab-treated rats. Our study indicates that bevacizumab-induced brain infiltration is driven by vascular endothelium and depends on PLXDC1 activation of tumor cells.

Molecular Cancer Biology

What's new?

Bevacizumab, a VEGF-targeting monoclonal antibody, has been observed to trigger an infiltrative growth pattern in glioblastoma as an escape mechanism. The mechanisms underlying this gliomatosis-like growth pattern, however, remain unclear. Here, the authors found that the infiltrative growth pattern occurs mostly along perivascular spaces and relies on the over-expression of PLXDC1 by tumor cells and on the restoration of the endothelial component of blood brain barrier. Altogether, the data show that the brain infiltration induced by bevacizumab is mainly driven by the vascular endothelium. Importantly, inhibition of PLXDC1 prevents bevacizumab-induced infiltrative growth, resulting in significant increase of survival.

Molecular Cancer Biology

Introduction

Glioblastoma (GBM), the most malignant primary brain tumor in adults, is a highly vascularized cancer. Standard-of-care treatment consists in surgery followed by chemo-radiation; nevertheless, the median survival is only 14.6 months due to tumor recurrence.[1] Advances in the molecular understanding of gliomagenesis have led to targeted therapies with one of the main targets being VEGF. VEGF and its receptors are highly expressed in both endothelial cells and GBM and VEGF mRNA up-regulation is triggered by hypoxia through stabilization of hypoxia-inducible factor-1.[2] Moreover, VEGF is produced by GBM stem-like cells (GSCs) in the vascular niche.[3–5] The importance of angiogenesis in maintenance and progression of GBM has prompted the development of bevacizumab, a monoclonal antibody against VEGF, which currently is the only FDA-approved targeted agent for recurrent GBM. However, results of recent trials with bevacizumab are openly discordant.[6–8] A sustained response to bevacizumab therapy is not the rule in GBM, whereas tumor regrowth after initial response is frequently seen, suggesting resistance mechanisms and secondary re-angiogenesis after transient normalization of tumor vessels. In addition, treatment with bevacizumab may trigger a phenotypic change in GBM that acquires a gliomatosis-like growth pattern.[9–11] Though its actual prevalence has been questioned, the infiltrative growth of GBM after bevacizumab treatment is described in several studies both on clinical[11–15] and on pathological basis.[9,16,17] Glioblastoma is thought to escape from antiangiogenic treatment using two mechanisms, a proangiogenic evasion, in which the tumor upregulates alternative proangiogenic pathways, and a proinvasive shift, in which the tumor modifies its phenotype and propagates to distant sites without reinitiating angiogenesis.[18] On magnetic resonance imaging (MRI), proangiogenic evasion manifests as nodular contrast-enhancing regrowth at the initial site of disease, whereas the proinvasive shift is recognizable by nonenhancing, fluid-attenuated inversion recovery (FLAIR)-bright areas without signs of revascularization (Figs. 1a and 1b). Here, we analyzed a surgically resected GBM that recurred after treatment with bevacizumab and that showed an infiltrative growth pattern on MRI. Pathological data from this specimen were exploited to set up orthotopic models of fluorescent human GBM xenografts that allowed us to dissect morphologically and molecularly the infiltrative growth induced by bevacizumab.

Materials and Methods

Clinical material

A surgical specimen of temporal lobe was fixed in formalin and paraffin-embedded. Four-μm thick paraffin sections were dewaxed with xylene and rehydrated in ethanol. Combined immunophenotyping with antibody antihuman CD31 (Monoclonal Mouse, clone JC70A, 1:50 dilution, Dako, Milan, Italy) and fluorescence *in situ* hybridization (FISH) using LSI EGFR Probe (Vysis EGFR/CEP7 FISH Probe Kit, Abbott, Rome, Italy) was performed as described (Supporting Information Methods).[19] Sections were incubated overnight at 4 °C in PB with 0.3% Triton X-100 and 0.1% NDS with Lectin from *Lycopersicon esculentum* (tomato) biotin conjugate (1:500; Sigma-Aldrich, St. Louis, MO) together with Monoclonal Mouse Anti-IDH1 (R132H; clone HMab-1, 1:50, Sigma Aldrich, St. Louis, MO). Monoclonal Rat Anticollapsin Response-Mediated Protein 5 (CRMP5, 1:50, Millipore, Billerica, MA) antibody was also used to stain GBM cells.[20] Slides were counterstained with DAPI (Vectashield mounting medium with Dapi, Vector Laboratories). Images were captured using a Laser Scanning Confocal Microscope (IX81, Olympus Inc, Melville, NY).

Culture of tumor cells and lentiviral infection

The U87MG human GBM cell line was purchased from the American Type Culture Collection (Manassas, VA). A patient-derived GSC line, namely the GSC1 cell line, was also used.[5] Cells were cultured and virally transduced for green fluorescent protein (GFP) and m-Cherry expression, and for PLXDC1 over-expression/down-regulation as described in Supporting Information Methods.

Cell growth and migration

For proliferation assay, GFP, PLXDC1-GFP and shPLXDC1-GFP U87MG cells were plated at density of 8×10^3/mL in 96 well plates in triplicate. Cell proliferation and migration were evaluated as described in Supporting Information Methods.

Invasion assay on endothelial cords

An *in vitro* co-culture system containing a feeder layer of adipose-derived stem cells (ADSCs), which are similar to mesenchymal stem cells, and endothelial colony forming cells (ECFCs), a subtype of umbilical cord blood-derived endothelial cells which can form vascular networks, was used to analyze motility and invasion of U87MG cells (Supporting Information Methods).[21]

Intracranial xenografts of fluorescent U87MG or GSC1 cells

Experiments involving animals were approved by the Ethical Committee of the Università Cattolica del Sacro Cuore (UCSC), Rome (Pr. No. CESA/P/51/2012). Immunosuppressed athymic rats (male, 250–280 g; Charles River, Milan, Italy) were anesthetized with intraperitoneal injection of diazepam (2 mg/100 g) followed by intramuscular injection of ketamine (4 mg/100 g). Animal skulls were immobilized in a stereotactic head frame and a burr hole was made 3 mm right of the midline and 2 mm anterior to the bregma. The tip of a 10 µL-Hamilton microsyringe was placed at a depth of 5 mm from the dura and 2×10^4 of either m-Cherry+ or GFP+ U87MG or GFP+ GSC1 cells were slowly injected. After grafting, the animals were kept under pathogen-free conditions and observed daily for neurological signs. Treatment with bevacizumab (10 mg/kg i.p. twice weekly) was initiated 4 days and 12 weeks after implantation in the rats grafted with U87MG and GSC1 cells, respectively. Control animals were treated with isotype IgG. After survivals ranging from 14 days to 16 weeks, the rats were deeply anesthetized and transcardially perfused with 0.1 M PBS (pH 7.4) then treated with 4% paraformaldehyde in 0.1 M PBS. The brain was removed and stored in 30% sucrose buffer overnight at 4 °C.

Fluorescence microscopy and immunofluorescence of brain tumor xenografts

The brains were serially cryotomed at 40 µm on the coronal plane. Sections were collected in distilled water and mounted on slides with Vectashield mounting medium (Bio-Optica, Milan, Italy). Images were acquired with a laser scanning confocal microscope (LSM 500 META, Zeiss, Milan, Italy). The cranio-caudal extension of the brain tumor was assessed on serial coronal sections. The tumor volume was determined as described.[21] For immunofluorescence, sections were blocked in PB with 10% BSA, 0.3% Triton X-100 for 45 min and incubated overnight at 4 °C with primary antibodies in PB with 0.3% Triton X-100 and 0.1% normal donkey serum (NDS). Monoclonal antibodies used were as follows, mouse antirat blood–brain barrier (Clone SMI-71) (1:500; Biolegend, San Diego, CA), mouse antihuman smooth muscle actin (Clone 1A4) (1:1000, DAKO Agilent, Santa Clara, CA). Polyclonal antibodies used were as follows, goat anti-CD34 (C-18) (1:50; Santa Cruz biotechnology, Dallas, TX), rat antimouse CD31 (1:100) (BD Bioscience, Franklin Lakes, NJ), rabbit anti-GFAP (1:1000; Dako Italia, Milan, Italy). For detecting brain microvessels, sections were incubated overnight at 4 °C in PB with 0.3% Triton X-100 and 0.1% NDS with Lectin from *Lycopersicon esculentum* (tomato) biotin conjugate (1:500; Sigma-Aldrich, St. Louis, MO) together with primary antibodies. Slices were rinsed and incubated in PB containing 0.3% Triton X-100 with secondary antibodies for 2 h at RT. Secondary antibodies used were as follows: Alexa Fluor 647 or 555 or 488 donkey antimouse, Alexa Fluor 488 or 555 or 647, donkey antirabbit secondary antibodies (1:500; Thermo Fisher Scientific,

Waltham, MA), Alexa Fluor 488 or 555 donkey antigoat antibodies (1:400; Thermo Fisher Scientific, Waltham, MA), Cy3 donkey antirat (1:200, EMD Millipore, Billerica, MA). For lectin immunostaining, sections were incubated for 2 h at RT in PB containing 0.3% Triton X-100 with streptavidin protein, DyLight 405 conjugate or streptavidin Alexa Fluor® 647 conjugate (1:200; Thermo Fisher Scientific, Waltham, MA). Before mounting, slices were incubated with DAPI (1:4000; Sigma-Aldrich) for 10 min. Immunofluorescence was observed with a laser confocal microscope (SP5; Leica) and images were acquired. Image analysis was performed with Leica Application Suite X software.

Gene expression profiling of U87MG cells after *in vivo* treatment with bevacizumab

Twenty-eight days after grafting, the brains treated either with bevacizumab (10 mg/kg i.p. twice weekly) or with isotype IgG were removed and mechanically dissociated to obtain single cell suspensions. The fluorescent m-Cherry U87MG cells were isolated by using FACSAria cell sorter (BD Biosciences, Milan, Italy). Total RNA was extracted from cells using TRIzol reagent (Life Technologies Corporation), labeled and hybridized to the Affymetrix GeneChip1.0ST array (Affymetrix, Santa Clara, CA) according the manufacturer's instructions. Gene expression analysis was performed on two samples for each group (bevacizumab *vs.* isotype IgG treated rats) from two independent experiments. Data preprocessing prior to the formal statistical analysis involved standard processes of normalization [robust Multi-array Average (RMA) method]. All data analysis was performed with R (http://www.R-project.org) using Bioconductor.[22] Differentially regulated genes were determined with LIMMA[23] applying default parameters and a FDR-corrected *p* value cutoff <0.05. Generation of the unified dataset involved through two consecutive steps. Gene set enrichment analysis was based on MSigDB using the GSEA online tool[24] hosted by the Broad Institute (http://www.broadinstitute.org/gsea/index.jsp).

Real-time quantitative PCR

Total RNA was isolated from shCNTR-GFP and shPLXDC1-GFP U87MG cells, and from GSC1 cells using TRIzol reagent (Life Technologies Corporation). PrimePCR™ precasted 96-well EMT pathway plate was purchased from Bio-Rad (Bio-Rad Laboratories, Inc. Hercules, CA). One microgram of RNA was reverse-transcribed into cDNA using iScript cDNA Synthesis Kit from Bio-Rad, according to the manufacturer's instructions. Real-time qPCR reactions were carried out as described by Bio-Rad in the PrimePCR™ instruction manual, including experimental control assays for reverse transcription (PrimePCR™ Reverse Transcription Control SYBR1 Green Assay), genomic DNA (PrimePCR™ DNA Contamination Control SYBR1 Green Assay), RNA quality (PrimePCR™ RNA Quality SYBR1 Green Assay) and PCR performance (PrimePCR™ Positive Control SYBR1 Green Assay). RT-PCR was performed on a CFX96 Touch Real-time PCR Detection System (Bio-Rad) using SsoAdvanced™ Universal

Molecular Cancer Biology

SYBR1 Green Supermix. The data were analyzed using the Bio-Rad CFX manager 3.1 software system. The samples were normalized against 3 reference genes; actin beta (ATCB), hypoxanthine phosphoribosyltransferase 1 (HPRT1) and glyceraldehyde-3-phosphate dehydrogenase (GAPDH).

Statistical analysis

Statistical significance was assessed by a two-tailed Student t-test with equal variance compared to the data obtained for saline controls. Statistical significance was assigned to p values <0.05.

Results

Bevacizumab-induced infiltrative growth of human GBM exploits the perivascular space

A surgically resected temporal lobe was assessed by histology and fluorescence microscopy. This 31-year-old man had undergone a first craniotomy in January 2009 at another institution for partial removal of a right parietal GBM (WHO IV). After surgery, he received radiotherapy and temozolomide according to the Stupp protocol.[1] A second craniotomy was performed in October 2009 at our center for local tumor recurrence (Fig. 1b, top left). Histology confirmed the diagnosis of GBM. On pathological analyses, Ki-67 labeling index was 20%, O^6-methylguanine-DNA methyltransferase promoter was unmethylated, EGF receptor (EGFR) was amplified, EGFR variant III was expressed, and isocitrate dehydrogenase (IDH)-1 was mutated. After the second craniotomy, due to residual enhancing tissue adjacent to the lateral ventricle, antiangiogenic treatment with bevacizumab was initiated (Avastin®, 10 mg/kg i.v. every 2 weeks in 6-week cycles) (Fig. 1b, top right). By the third cycle of bevacizumab, follow-up MRI showed reduction of the paraventricular area of contrast enhancement, however, the right temporal lobe appeared swollen due to diffusely infiltrating tissue that did not enhance after administration of contrast medium (Fig. 1b, bottom left). In January 2011, due to headache and poorly controlled seizures, a third craniotomy was performed with resection of the right temporal lobe in an en bloc fashion. Histological examination showed an increased cell density due to enlarged cells with atypical nuclei, which were mainly located along the perivascular spaces (Fig. 1b, bottom right). Fluorescence microscopy combining immunohistochemistry for CD31 and FISH for EGFR showed that a substantial fraction of tumor cells with amplified EGFR signals lied close to CD31-expressing endothelial cells (Fig. 1c). In tumor regions as far as 12 cm from the primary neoplasm, we calculated a 7:5 ratio between the tumor cells that were spatially associated with the vascular endothelium and those that were not. These results were confirmed by fluorescence microscopy combining anti-IDH1 or anti-CRMP5 immunostaining, which selectively labeled the tumor cells,[20] either with lectin staining of the blood vessels or with anti-CD31 immunofluorescence, that selectively stains the endothelial cells (Fig. 1d). Using these techniques, we confirmed the perivascular tumor growth in the nonenhancing FLAIR-hyperintense temporal lobe. However, in this region we did not recognize morphological patterns of vascular mimicry and vessel cooption, which were seen in the specimen obtained at surgery for tumor recurrence in the parietal region, i.e., at the site of primary surgery (Supporting Information Fig. S1). Taken together, these studies demonstrate that the perivascular spaces are preferential routes for tumor spreading in bevacizumab-induced infiltrative shift of GBM.

Effect of bevacizumab on the invasive behavior of U87MG cells in vitro

Based on the histologic data of our patient, we hypothesized that the infiltrative shift occurring after bevacizumab therapy for GBM may involve changes in the perivascular environment that would become more permissive to the invading cells. Then, we aimed to reproduce in vitro conditions that mimic the in vivo interactions between GBM cells and perivascular environment using an invasion assay on endothelial cords.[21] The human U87MG cell line was chosen because its growth depends on angiogenesis and VEGF signaling.[25,26] Cords of human ECFCs were established using an in vitro colony formation assay, and GFP expressing U87MG cells, pretreated with 2.5 mg/mL of either IgG or bevacizumab for 72 h, were seeded in the top chamber of a cell invasion assay. Both the top and bottom chambers were also treated with either IgG or bevacizumab (final concentration 2.5 mg/mL). We found that the presence of U87MG cells resulted in marked increases in connected tube area of established cords, both in wells that received IgG-pretreated U87MG cells and in those with bevacizumab-pretreated U87MG cells (Supporting Information Fig. S2A). Interestingly, the U87MG cells invaded through the matrix of the chamber. At 48 h post seeding, bevacizumab-pretreated cells exhibited a slightly higher invasive growth compared to IgG-pretreated cells, when the co-culture was used as the "chemoattractant" (Supporting Information Fig. S2B). Bevacizumab-pretreated U87MG cells indicated a tendency to line up adjacently to the endothelial cords, though there was not a significant overlap of U87MG cells with the cords, as assessed by automated image analysis (Supporting Information Fig. S2C). These findings suggest that in an in vitro model system, bevacizumab increased the tropism of U87MG cells toward the vascular endothelium, however, it did not significantly enhance migration along the endothelial cord surface.

Effect of bevacizumab on the invasive growth of U87MG brain xenografts

In the attempt to reproduce the complex environment in which bevacizumab induces the infiltrative growth of GBM, we grafted fluorescent U87MG cells (expressing either m-Cherry or GFP) onto the striatum of athymic rats and assessed the effects of bevacizumab (10 mg/kg i.p. twice weekly for 3 weeks) on the growth pattern of tumor xenografts. Three weeks after brain grafting, isotype IgG treated control rats showed compact tumor masses with sharply defined edges (Figs. 2a and 2b). At this time, the rats developed clinical signs, including >20%
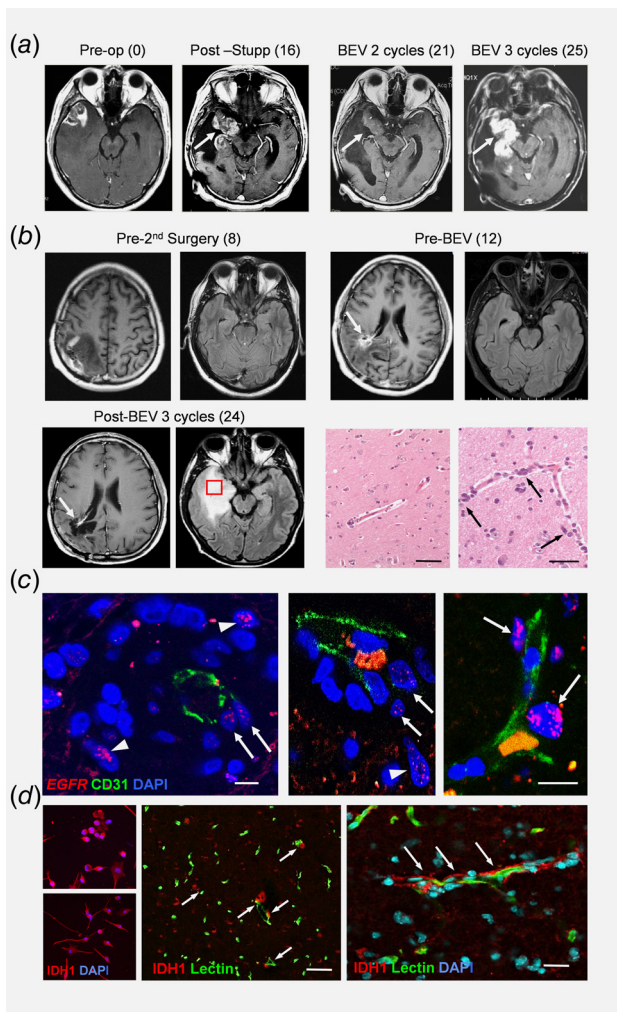
Figure 1. Radiological and morphological assessment of bevacizumab treatment on recurrent GBM. (*a*) Magnetic resonance (MR) imaging (T1-weighted Gd enhanced) showing an illustrative case of response to bevacizumab and late tumor regrowth (*arrows*, recurrent tumor; in *brackets*, follow-up in months). (*b*) Axial Gd-enhanced T1-weighted MR imaging of reported case (*upper panel*). Twelve months after primary surgery, an area of contrast enhancement developed adjacent to the lateral ventricle (*arrow*). The right temporal lobe showed normal FLAIR signal. After bevacizumab therapy (*lower panel*), the contrast enhanced area in the right para-ventricular region disappeared (*left; arrow*), however, the right temporal lobe swelled due to hyper-intense diffusely infiltrating lesion on FLAIR sequence (in *brackets*, follow-up in months). Histological picture (*lower panel, right*) of the resected temporal lobe (brain region framed in FLAIR image). The temporal lobe parenchyma appears infiltrated by rare cells with atypical nuclei that are in close relationship with the capillaries (*arrows*). H&E. Scale bars, 150 μm (*left*) and 70 μm (*right*). (*c*) Combined anti-CD31 immunohistochemistry and FISH for the EGFR probe showing the tumor cell nuclei with amplified EGFR signals either isolated (*arrowheads*) or in close relationship with CD31+ endothelial cells (*arrows*). Scale bars, 10 μm. (*d*) Immunofluorescence with anti-IDH1 antibody for selective staining of tumor cells combined with lectin staining of vascular structures. Validation of IDH1 immunoreaction on primary cell cultures of patient-derived IDH1 mutated GBM (*left panels*). The infiltrating IDH1-positive tumor cells (*red*) lie in close proximity with vessels along the perivascular spaces (*arrows*). Scale bars, 150 μm (*left*) and 40 μm (*centre* and *right panels*).

weight loss, spastic gait, and lethargy. Analysis of the tumor margins did not reveal regions of brain infiltration. Occasionally, the tumor border showed irregular profiles (Fig. 2*b*, *right panel*), which occurred in proximity of the rhinal fissure and likely resulted from the passive resistance offered by arachnoid or vascular structures. Only rare were tumor cells scattered in the brain up to a maximal distance of 660 μm from the tumor margin (Fig. 2*c*). Lectin staining for endothelial structures showed that capillaries and venules crossing the brain-tumor interface were surrounded for short distances by a few tumor cells (Fig. 2*d*). Bevacizumab-treated tumors were significantly smaller than controls (Fig. 2*e*). Three weeks after grafting, the tumor volume was 116.5 ± 23.1 mm^3 (mean $\pm$ sem, $n = 3$) and 17.7 ± 2.5 mm^3 (mean $\pm$ sem, $n = 3$) in control and bevacizumab-treated tumors, respectively ($p < 0.02$; Student-t test). However, the latter tumors showed deposits on the walls of the ventricles (Fig. 2*e*, arrows). The margins of bevacizumab-treated tumors were quite irregular due to bands or islands of tumor cells that spread onto the surrounding brain (Fig. 2*f*). Analysis of brain regions surrounding the tumor revealed that the tumor cells arranged themselves to form multiple shaped structures including, satellites, multilayered columns, chain-like files, and isolated cells. Satellites and multilayered columns are likely to represent different aspects of vessel cooption, a process whereby the tumor cells organize themselves into cuffs around microvessels. The chains of cells in single file likely reflect an acquired attitude of the tumor cells to form tubular structures, a phenomenon referred to as tubulogenesis. Isolated cells demonstrated enhanced potential of the tumor for cell motility and brain invasion. Three weeks after grafting, the distance traveled by the tumor cells through the brain was significantly longer in bevacizumab-treated rats than in control ones ($p < 0.001$; Student-t test) (Figs. 2*c* and 2*g*). In bevacizumab treated xenografts, tumor satellites and multilayered columns were always associated with endothelial structures, thus confirming that they resulted from vessel cooption. The chain-like arrangement of tumor cells featured mosaic tubule formation reminiscent of vascular mimicry (Fig. 2*h*). Isolated tumor cells exhibited elongated morphology and a strict tropism for the endothelial elements (Fig. 2*h* and Supporting Information Fig. S3). Bevacizumab significantly reduced microvessel density in the xenografts (Fig. 2*i*, *left panel*). By 28 days after grafting, in bevacizumab-treated xenografts 85.7% of tumor cells that lied farther than 500 μm from the tumor margin had established cell-to-cell interactions with endothelial elements (Fig. 2*i*, *right panel*). Therefore, the orthotopic U87MG grafting model did reproduce the bevacizumab-induced infiltrative shift of human GBM confirming that this phenomenon occurs mostly along the perivascular spaces.

Molecular changes induced by bevacizumab on U87MG cells *in vivo*

Grafting of fluorescent GBM cells provides the opportunity to retrieve selectively the tumor cells from the brain by FACS and

to analyze the molecular changes elicited by bevacizumab *in vivo*. Analyzing the molecular changes of GBM under *in vivo* conditions is of paramount importance, since transcriptional regulators that enable cells to proliferate in the tumor microenvironment *in vivo* are nonoverlapping with those required *in vitro*.[27] To this aim, athymic rats grafted with fluorescent U87MG cells were treated with bevacizumab (10 mg/kg i.p. twice weekly for 3 weeks). Three weeks later, their brains were removed,

fluorescent cells were sorted, and their gene expression profile was compared to that of tumor cells sorted from isotype IgG treated control xenografts. Results of gene expression analysis showed that the highest modulated genes were those involved in epithelial to mesenchymal transition (EMT) and hypoxia (Fig. 3*a*). Among the highest modulated genes, we found the receptor Plexin Domain Containing 1, PLXDC1 (or Tumor Endothelial Marker-7, TEM-7), a trans-membrane protein
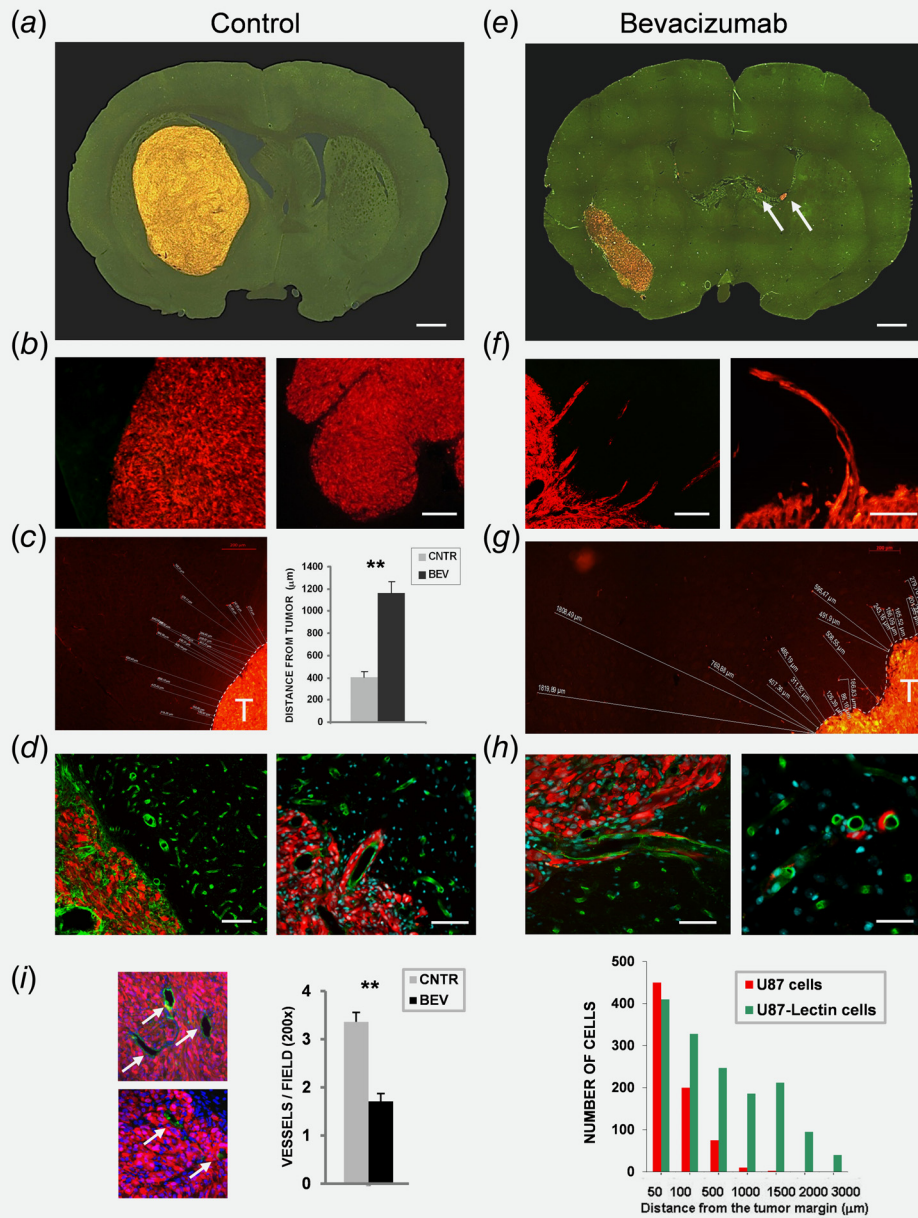

FIGURE 2. Legend on next page

known to be expressed by GBM associated endothelial cells.[28,29] TGF-β1, extracellular matrix remodeling genes, and several others which define the mesenchymal signature were found significantly up-regulated after *in vivo* treatment with bevacizumab as compared to isotype IgG treated U87MG cells (Supporting Information Table S1).

To assess the role of PLXDC1 in bevacizumab-induced infiltrative shift, we over-expressed and down-regulated this receptor in U87MG cells (PLXDC1-GFP U87MG and shPLXDC1-GFP U87MG, respectively). Over-expression and down-regulation of PLXDC1 was verified by RT-PCR and flow cytometry (Fig. 3b). *In vitro*, PLXDC1-GFP U87MG cells exhibited increased proliferation and migration whereas shPLXDC1-GFP U87MG cells showed decreased proliferation and migration as compared to control GFP U87MG cells (Fig. 3b). We then grafted PLXDC1-GFP U87MG and GFP U87MG cells onto the striatum of athymic rats. As expected, control GFP U87MG cells developed compact tumors with sharp margins (Fig. 3c, right). Xenografts arising from PLXDC1-GFP U87MG cells exhibited profiles suggesting vessel cooption (Fig. 3c, left). Then, over-expression of PLXDC1 in U87MG cells elicited vessel cooption, although it was not sufficient *per se* to trigger all the repertoire of brain invasion induced by bevacizumab.

Effect of bevacizumab on the growth of GSC brain xenografts

To validate the effect of bevacizumab on perivascular spreading of GBM cells and the role of PLXDC1 in this process, we developed brain xenografts of patient-derived GSCs, which are known to closely mimic the human tumor. To this purpose, 12 weeks after grafting GFP-expressing GSC1 cells onto the striatum of athymic rats, we administered bevacizumab (10 mg/kg i.p. twice weekly) for 3 weeks. One week after the end of treatment, we compared their brains with those of isotype IgG treated control rats. Differently from the U87MG cells, GSC1 cells developed highly infiltrating tumors (Supporting Information Fig. S4A). Tumor cells invaded the homolateral striatum and piriform cortex and extended contralateral through the

corpus callosum, anterior commissure, septal nuclei, and optic chiasm. Brain invasion occurred mostly along these axonal paths, however, a remarkable fraction of tumor cells traveled along the perivascular spaces (Supporting Information Fig. S4B-C). In spite of reduction of tumor cell density in the grafted striatum and subcortical white matter, bevacizumab did not inhibit the growth of GSC1 tumors to the same extent as in U87MG xenografts (Supporting Information Fig. S4D). However, bevacizumab strongly increased perivascular spreading of GSC1 cells (Supporting Information Fig. S4E-F). In some areas, GSC1 cells completely encased the blood vessels in a parasitic manner. We then interrogated whether PLXDC1, that was heavily involved in the response of U87MG cells to bevacizumab, may also play a role in GSCs. To this aim, we performed Real-Time PCR analysis of GSC1 cells retrieved from the brain of rats treated with bevacizumab or with isotype IgG. Results showed that, as compared to IgG treated controls, PLXDC1 mRNA increased by 2.1 times in GSC1 treated with bevacizumab (Supporting Information Fig. S4G). These data support the concept that bevacizumab enhances perivascular growth of GBM cells and that PLXDC1 does have a role in this process.

PLXDC1 as target against the bevacizumab-induced infiltrative shift of U87MG cells

To establish the actual role of PLXDC1 in bevacizumab-induced infiltrative shift and to explore its potential value as therapeutic target, brain xenografts were established using shPLXDC1-GFP U87MG cells and the rats were treated with bevacizumab (10 mg/kg i.p. twice weekly for 3 weeks). Controls included either rats grafted with scrambled shRNA (shCNTR)-GFP U87MG cells and treated with isotype IgG, rats grafted with scrambled shCNTR-GFP U87MG cells and treated with bevacizumab, or rats grafted with shPLXDC1-GFP U87MG cells and treated with isotype IgG. Three weeks after grafting, tumor xenografts arising from shPLXDC1-GFP U87MG cells that received bevacizumab were significantly smaller than all control groups ($p < 0.002$; Student *t*-test) and did not show perivascular spreading (Figs. 4a–4c). Importantly, the rats

Figure 2. Tumor xenografts generated by m-Cherry expressing U87MG cells implanted in the brain of athymic rats and treated with bevacizumab or isotype IgG. (*a*) By 28 days after grafting, in control IgG-treated rats the tumor appears as a compact mass with sharply defined edges. Scale bar, 1 mm. (*b*) Analysis of the tumor margins does not reveal regions of brain infiltration. Occasionally, the tumor margin may show an irregular profile. This occurs as the tumor approaches the rhinal fissure and likely results from the passive resistance offered by arachnoidal structures. Scale bar, 70 µm. (*c*) Higher magnification view showing single tumor cells in the brain up 650 µm from the tumor margin (*T, tumor*). Bar graph showing the distance traveled into the brain by control and bevacizumab-treated tumor cells (**, $p < 0.01$). (*d*) Staining of vascular structures with lectin (*green*) demonstrates a few tumor cells that surrounded capillaries and venules at the brain-tumor interface. Scale bars, 100 µm. (*e*) Bevacizumab-treated tumor xenografts are smaller than controls, however, metastases spread along the CSF pathways (*arrows*). Scale bar, 1 mm. (*f*) Tumor cells arranged in satellites, finger-like extensions, and chain-like files. Scale bar, 70 µm. (*g*) Isolated tumor cells are scattered in the peritumor tissue for considerable distances. H, Both at the margin and far from the tumor bulk, the m-Cherry U87MG cells show a strict tropism for the vascular endothelial cells (*green*, lectin). Scale bars, 50 µm. (*i*) Micro-vessel density is significantly lower in bevacizumab-treated xenografts (*bottom left panel, arrows*) as compared to control IgG-treated ones (*upper left panel, arrows; green*, CD31 immunostaining). In bevacizumab-treated tumors, the U87MG cells that established cell-to-cell interactions with endothelial elements had spread through the brain for much longer distances than those U87MG cells that were not spatially associated with the lectin-positive cells (*right panel*).
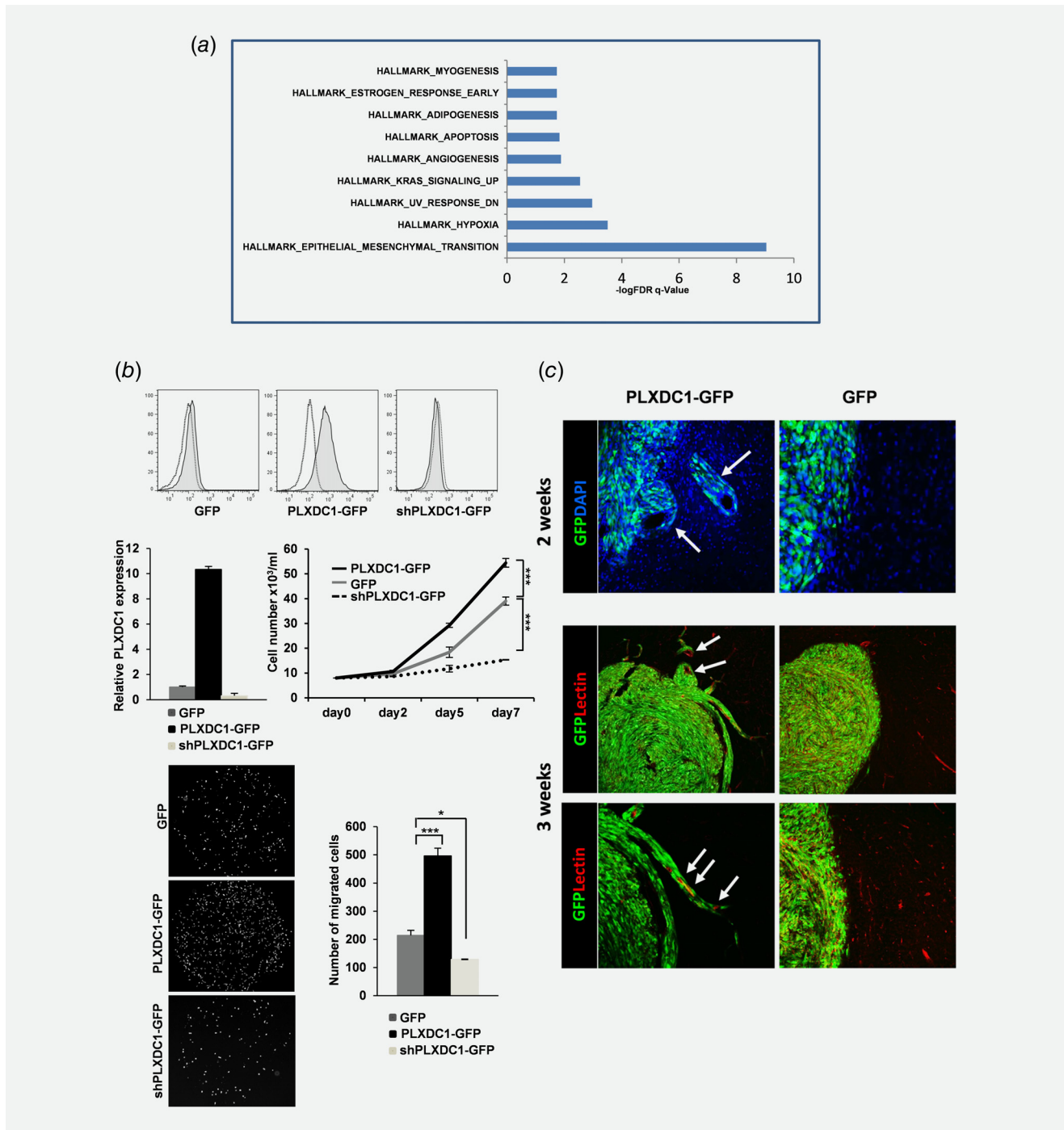
Figure 3. Molecular changes elicited by bevacizumab *in vivo* on U87MG cells and effects of PLXDC1 over-expression. (*a*) GSEA of highly modulated genes as assessed by gene expression array on U87MG cells retrieved from the brain of bevacizumab treated rats compared to IgG treated controls. (*b*) FACS analysis (*upper panel*), RT-PCR analysis and proliferation assay (*middle panel*), and migration assay (*lower panel*) of control GFP, PLXDC1-GFP and shPLXDC1-GFP U87MG cells. (*c*) *In vivo* effects of PLXDC1 over-expression. Brain xenografts of GFP U87MG and PLXDC1-GFP U87MG cells showing perivascular growth (*arrows*; U87MG cells, *green*; lectin, *red*). Xenografts of control U87MG cells do not infiltrate the brain.

grafted with shPLXDC1-GFP U87MG cells and treated with bevacizumab survived significantly longer than other groups, including rats grafted with shPLXDC1-GFP U87MG and treated with isotype IgG ($p = 0.002$, log rank test; Fig. 4*c*). These

results demonstrate that PLXDC1 downregulation is not sufficient *per se* to inhibit the growth of U87MG brain xenografts but can exert an inhibitory effect in conditions of reduced availability of VEGF, like bevacizumab therapy.

PLXDC1 alters the expression pattern of epithelial and mesenchymal markers in U87MG cells

To investigate more in details the molecular mechanisms through which PLXDC1 modulates the perivascular spreading of U87MG, the expression of several mesenchymal and epithelial marker genes was carried out by RT-PCR analysis on shPLXDC1-GFP and shCNTR-GFP U87MG cells. The mRNA levels of epithelial transcripts, such as *E*-cadherin (CDH1) and Keratin 14 (KRT14) were significantly increased, whereas mesenchymal marker genes, such as vimentin (VIM), TGFB1, TGFB 2 and TGFB 3, occludin (OCLN), and ZEB1 and ZEB2 among others, were significantly reduced in shPLXDC1-GFP U87MG cells compared to shCNTR-GFP U87MG cells (Supporting Information Fig. S5). These results suggest that PLXDC1 silencing inhibits the EMT program induced by bevacizumab.

Relationships of U87MG tumor cells, astrocyte endfeet, and blood brain barrier (BBB)

Taken together, our results indicate that in response to bevacizumab the U87MG cells, which possess a poor intrinsic ability to invade the brain, become able to migrate using the perivascular spaces as route for spreading. This invasive behavior depended on the up-regulation of PLXDC1 triggered by bevacizumab. Then, we focused on the cell components of perivascular environment. In the brain, the vascular endothelium is covered by astrocytic endfeet that may pose an obstacle to glioma cells invading along blood vessels.[30] Theoretically, perivascular glioma cells may either travel outside the astrocytic endfeet, thereby preserving the BBB, or disrupt astrocyte covering through the elimination of endfeet and BBB. In order to dissect morphologically the relationships between glioma cells, astrocytes, and brain endothelium, we used fluorescently labeled U87MG cells and type-specific markers. Astrocytes and BBB were assessed by anti-GFAP and anti-SMI71 immunohistochemistry, respectively (Fig. 5, *Normal*). The latter marker stains selectively the endothelial component of the rat BBB.[31] In control isotype IgG treated U87MG brain xenografts, SMI71 immunostaining was nearly absent in vessels lying within the tumor and in peritumor regions up to about 500 μm from the tumor margin (Fig. 5, *IgG*). In this region, perivascular spreading of tumor cells was quite infrequent and, where present, occurred along vessels that lacked or showed poor SMI71 staining. Conversely, bevacizumab-treated xenografts displayed U87MG cells that had traveled along vessels with positive SMI71 reaction (Fig. 5, *BEV*). As expected, bevacizumab partly restored the BBB in the peritumor regions. However, the normal interaction between the astrocytic endfeet and vasculature was disrupted by the elimination of the endfeet altogether, whereby the U87MG cells came in direct contact with endothelial cells that had partly restored SMI71 expression (Fig. 5, *BEV*). In brain xenografts of U87MG cells over-expressing PLXDC1 treated with isotype IgG, perivascular spreading occurred at short distances from the tumor bulk mostly as vessel cooption around vessels that lacked SMI71 (not shown). Notably, xenografts of shPLXDC1 U87MG cells treated with bevacizumab showed a dramatic reduction in perivascular spreading in spite of restored SMI71 staining (Fig. 5, *shPLXDC1 BEV*). Bevacizumab enhanced perivascular spreading around pericyte coverings, however, pericytes did not proliferate substantially in response to bevacizumab (not shown).

In order to invade the brain along perivascular spaces, the U87MG cells required PLXDC1 upregulation and restoration of the endothelial component of BBB. Importantly, inhibition of PLXDC1 prevented the bevacizumab-induced infiltrative shift of U87MG cells.

Discussion

Clinical and preclinical background of bevacizumab-induced infiltrative shift in GBM

Since the first reports on the use of bevacizumab in GBM, it became apparent that antiangiogenic therapy induces a modification of the clinical and radiological behavior of the tumor that assumes an infiltrating, nonenhancing gliomatosis-like growth pattern.[9,13,15] The tendency of recurrent GBM to behave more invasively after antiangiogenic treatment and the correlation between tumor invasiveness and hypoxia have been described in several studies.[16,17] However, some clinical studies have questioned the tendency of GBM to become more invasive after bevacizumab treatment.[12] In the randomized AvaGlio trial comparing standard therapy with or without bevacizumab, Wick *et al.* did not observe difference in growth patterns by MRI of newly diagnosed supratentorial GBM, including both contrast-enhancing and nonenhancing lesions.[32] However, in a more recent paper from the same group focusing on the patterns of GBM progression in the AvaGlio trial, a T2 diffuse infiltrative pattern was noticed in 12.4% of patients treated with bevacizumab and in 7.1% of patients treated with placebo,[33] suggesting that treatment with bevacizumab may indeed cause an increased number of diffusely infiltrating progressions.

On pathological examination, recurrent malignant glioma treated with bevacizumab show diffuse neuropil infiltration with upregulation of invasion markers.[9] It is worth noting, however, that these observations were from small stereotactic biopsies, assessed by conventional histology without any selective labeling of tumor cells. Conversely, we used the amplified *EGFR* signal, IDH1 mutation, and CRMP5 expression to trace selectively the infiltrating tumor cells through the temporal lobe of our patient and we were able to demonstrate that the perivascular spaces were preferential routes for the brain invasion after bevacizumab treatment. We did not recognize patterns of vascular mimicry as well as of vessel cooption. It should be noted, however, that the patient sample consisted of a temporal region with nonenhancing T2 diffuse infiltrative MRI signal lying as far as 12 cm from the site of primitive GBM. Vessel cooption and vascular mimicry occurred closer to the primary neoplasm, where tumor angiogenesis is much more prominent.

Robust preclinical data support the concept of increased invasiveness of GBM after antiangiogenic treatment and its relationship with vascular structures.[9–11,13,14,34–36] In orthotopic murine models of GBM treated with antiangiogenic drugs, the tumor cells invade perivascular spaces and form satellites separated from the primary
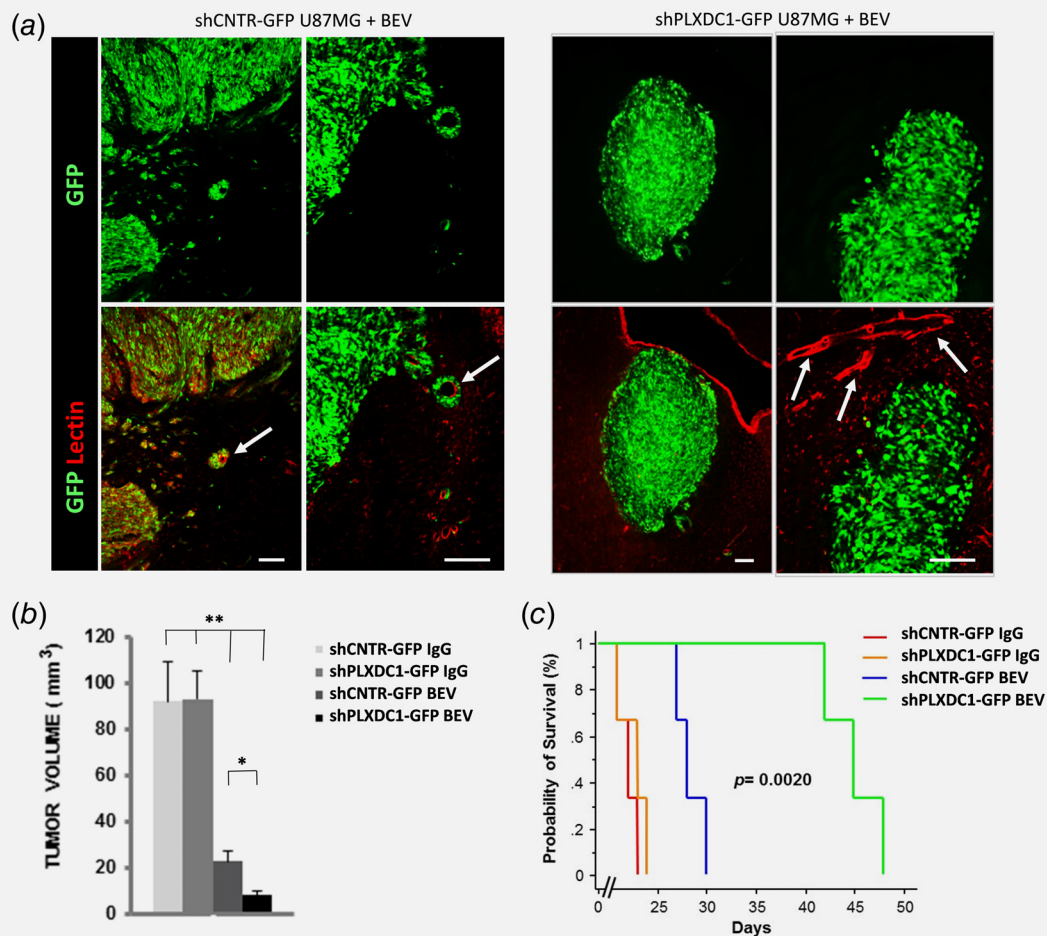
Figure 4. Inhibition of PLXDC1 expression in U87MG cells prevents bevacizumab-induced infiltrative growth of brain xenografts. (*a*) In rats grafted with shCNTR-GFP U87MG cells, bevacizumab treatment elicited an infiltrative growth in the perivascular spaces, as demonstrated by tumor satellites associated with endothelial structures (*arrows*). Rats grafted with shPLXDC1-GFP U87MG cells and treated with bevacizumab developed small nodular tumors with defined edges. Perivascular spreading does not occur around vessels lying close to the tumor margin (*arrows*). Scale bars, 100 µm. (*b*) Bevacizumab treatment significantly reduced tumor volume both in shPLXDC1-GFP and in shCNTR-GFP U87MG brain xenografts (*left panel*). The mere PLXDC1 inhibition does not affect significantly the volume of U87MG brain xenografts. (*c*) Rat survival is significantly increased in rats grafted with shPLXDC1-GFP U87MG cells that received bevacizumab (*right panel*).

tumor.[34,36] To investigate the effects of bevacizumab *in vivo*, the U87MG brain xenograft model has widely been used because it simulates the human condition showing a significant decrease in contrast enhancement on MRI.[37,38] Reportedly, bevacizumab inhibits tumor growth and prolongs survival of U87 brain xenografts.[39,40] In this model, the typical nodular growth pattern shifted toward an infiltrative one after bevacizumab therapy (Supporting Information Table S2). Satellite tumors and finger-like extensions in the brain of bevacizumab-treated animals result from the decreased supply of oxygen and nutrients that may act as a stimulus for tumor cell migration through up-regulation of invasion-related proteins.[14] The hypothesized mechanism for explaining the increased invasive behavior of the tumor after antiangiogenetic

therapy is cooption of existing brain vessels by the tumor to escape the blockade of VEGF-driven angiogenesis. It has been claimed that tumor hypoxia, which is induced by antiangiogenic therapy, activates proinvasive survival pathways.[10,11,14] In particular, the Src family of kinases (SFKs) may play a key role at the interface between intra and extracellular signals either regulating cell–cell adhesion, cell-ECM adhesion, and ECM invasion[41] or by catenin phosphorylation.[13]

Hypotheses for the infiltrative shift after bevacizumab therapy
Previous hypotheses for the infiltrative shift postulate that antiangiogenic treatments decrease oxygen and nutrient supply to
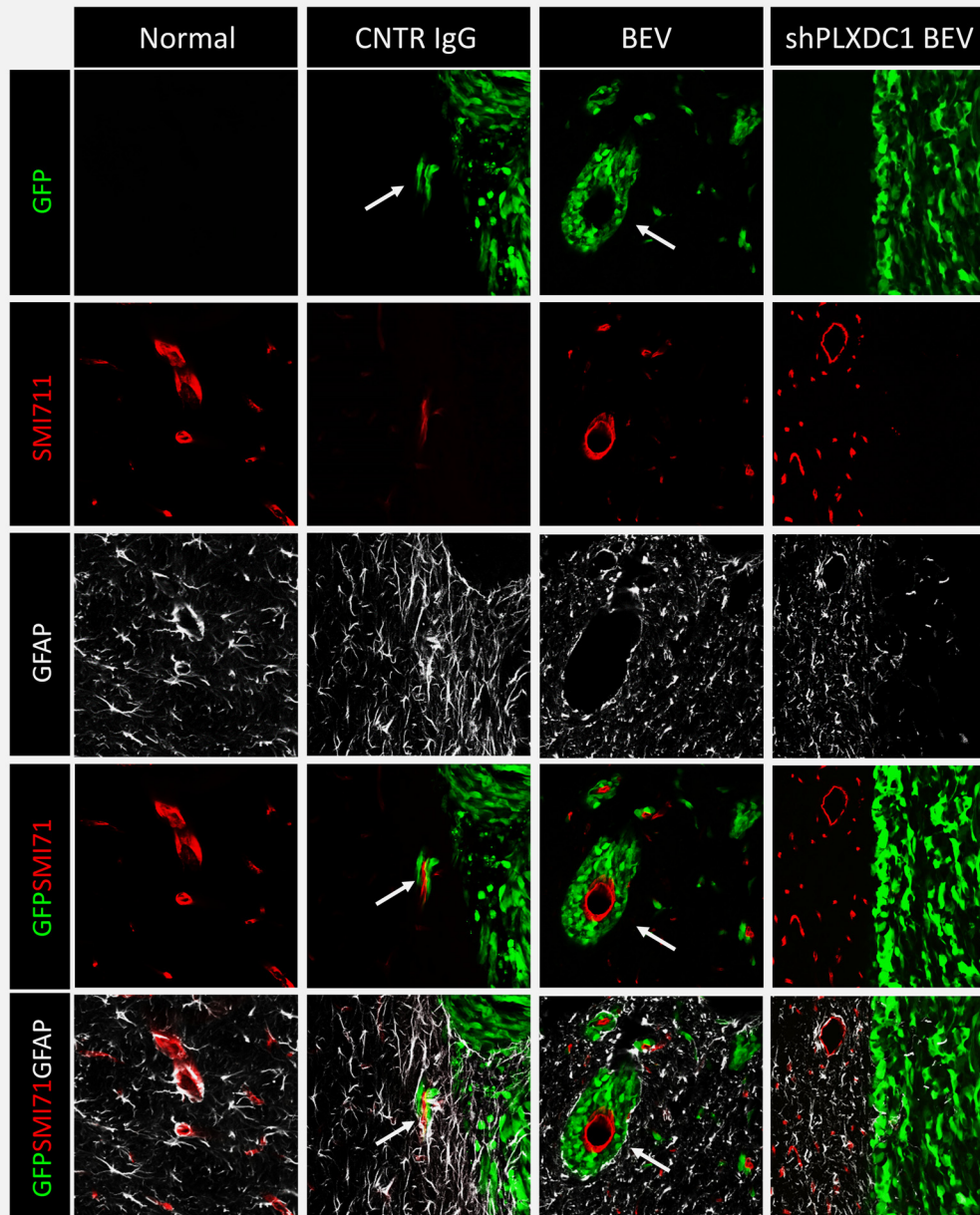
Figure 5. Assessment of relationships among U87MG tumor cells, astrocytes, and endothelial component of BBB (SMI71). In the brain of normal rats (*Normal*), the endothelial cells express SMI71 and are covered by the vascular endfeets of astrocytes. In control brain xenografts (*CNTR IgG*), which harbor GFP shCNTR-GFP U87MG cells and received IgG, only a few tumor cells cross the brain-tumor interface along the perivascular spaces with disruption of the astrocytic covering (*arrow*). Treating xenografts of shCNTR-GFP U87MG cells with bevacizumab (*BEV*) resulted in perivascular spreading. Cufs of tumor cells grew around brain vessels with restored SMI71 expression (*arrow*). The astrocytic endfeets are completely displaced by the tumor cells. Inhibition of PLXDC1 in GFP U87MG cells prevented the perivascular spreading induced by bevacizumab (*shPLXDC1 BEV*).

tumor cells that in turn activate hypoxia-triggered up-regulation of invasion-related proteins. The perivascular migration was explained as a prosurvival response of the tumor cells to hypoxia.

At morphological level, the infiltrative shift is characterized by vessel cooption, a phenomenon whereby the tumor cells migrate along the perivascular spaces to form multilayered sleeves. Vessel
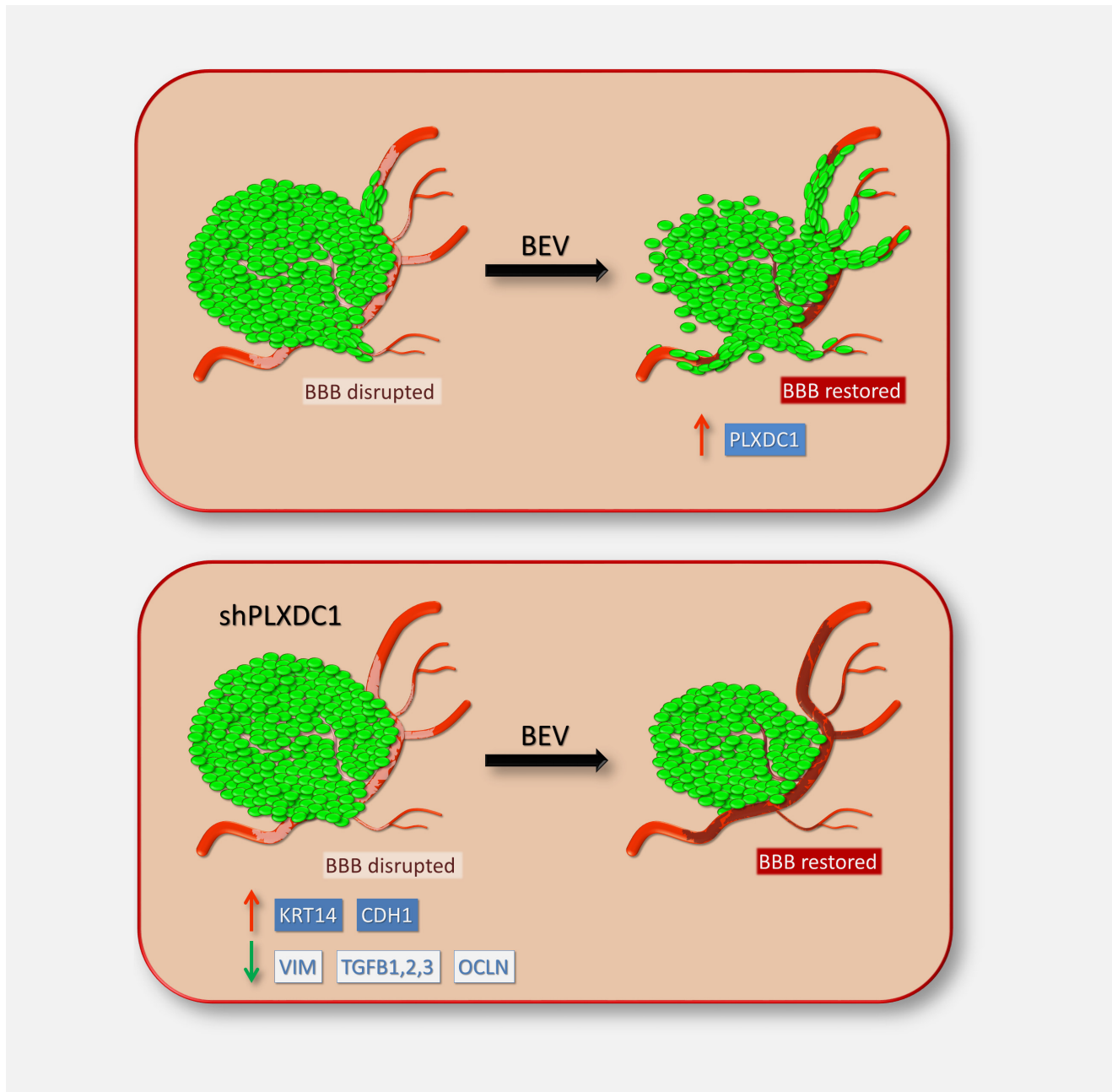
Figure 6. Schematic drawing of bevacizumab-induced infiltrative growth of GBM. Perivascular spreading of tumor cells is driven by the endothelium with restored BBB and requires activation of PLXDC1 *(upper panel)*. PLXDC1 silencing inhibits the vascular-like infiltrative behavior of GBM cells despite BBB restoration *(lower panel)*.

cooption generates histological pictures such as satellites and finger-like extensions depending on the cutting plane. However, it is important to note that previous *in vivo* studies did not label selectively the tumor cells, thus missing important aspects of the tumor changes induced by bevacizumab. In the present study, we used orthotopic xenografts of fluorescently labeled U87MG cells and selectively stained the brain vessels for endothelial cell markers, a technique that allows a much deeper dissection of the tumor/endothelial cell interactions. In addition to vessel cooption,

we were able to identify other behaviors of U87MG cells after *in vivo* treatment with bevacizumab that included, endothelium oriented migration, mosaic tubule formation, and niching with endothelial cells. Mechanistically, such a repertoire of vascular-like behaviors by tumor cells are difficult to specifically define as a pro survival response to hypoxia.

The interactions between tumor and endothelial cells elicited by bevacizumab resemble those described by Tsai *et al.* during migration of oligodendrocyte precursors cells (OPCs) along blood

vessels in the developing mammalian brain.[42] Glioblastoma cells share with OPCs marker expression and propensity to migrate over long distances. In addition, both GBM cells and OPCs require the vascular endothelium as a physical substrate for migration. Recently, Griveau *et al.* assigned a glial signature to brain xenografts of multi-passaged subcutaneous U87 tumors treated with bevacizumab because of increased levels of Olig2 and Nkx2.2, two transcription factors that are critical for oligo-dendrocyte differentiation.[43] On the other hand, Piao *et al.* described proneural to mesenchymal transition of U87 cells after treatment with bevacizumab that paralleled the increase in invasive characteristics on histological examination.[44] In contrast with studies based on xenograft models, Urup *et al.* reported that in patients' samples TGF-β1 and other genes defining the mesenchymal signature were inactivated at the time of progression.[45] They speculate that reduced hypoxia, as a consequence of bevacizumab-induced vascular normalization, may lead to TGF-β1 inhibition and thus reverse mesenchymal transition. However, clinical studies that analyzed GBM after treatment with bevacizumab describe a sarcomatous, spindle cell morphology with increased hypoxia markers.[46] In addition, after bevacizumab 33.3% GBMs transitioned from proneural or proliferative to mesenchymal, whereas 25% GBMs transitioned from mesenchymal to proneural.[47] More recently, brain invasion in U87 xenografts treated with bevacizumab was related with fibroblast growth factor 13 (FGF13).[35] Interestingly, though the bevacizumab-induced tumor invasion was remarkably decreased *in vivo* by FGF13 shRNA, the expression level of FGF13B was not changed by bevacizumab *in vitro*. Our study and our failure to reproduce the perivascular tumor growth induced by bevacizumab in *in vitro* models highlight one main limit of neuro-oncology research, whereby the incomplete nature of *in vitro* data may not fit with *in vivo* results. In the attempt to overcome this obstacle, we analyzed molecularly the tumor cells that were selectively retrieved from the brain of rats treated with bevacizumab, i.e., in the microenvironment where the tumor cells interact with other cell players of the brain.[27] In general, our results support the concept that bevacizumab elicits cell features, like spindle-shape and elongated morphology, typical of invading cells and that tumor spreading occurs along the perivascular spaces. We also described bevacizumab-related phenomena, such as tubule generation and niching with endothelial cells, previously reported in GBM stem cells as a result of their mesenchymal differentiation potentials.[5,48,49] In addition to a deeper morphological dissection of the infiltrative growth pattern, our methods demonstrate that the perivascular invasion induced by bevacizumab requires activation of PLXDC1. The exact function of this trans-membrane receptor is unknown. In the embryonic brain, PLXDC1 expression overlaps with the gene *PLXDC2*, which is more widespread across the brain and relates with members of the Wnt family that are involved in axonal guidance.[50] PLXDC1 binds to components of ECM[51,52] and is associated with tumor invasion in gastric cancer.[53] PLXDC1 was also been identified in a genome-wide expression screening of GBM endothelium[28] and was proposed as a possible target for therapeutic anti angiogenic intervention in cancer.[54]

In our study, the over-expression of PLXDC1 *per se* was able to change partly the growth features of U87MG cells, whereby they become able to travel for short distances *via* vessel cooption. More importantly, inhibition of PLXDC1 expression by shRNA prevented the bevacizumab-induced infiltrative growth of U87MG cells resulting in a significant increase of survival. Molecularly, PLXDC1 regulated the EMT program of tumor cells, whereby its silencing increased the mRNA levels of epithelial transcripts, whereas those of mesenchymal marker genes were reduced.

We also showed that the bevacizumab-induced brain invasion along perivascular spaces, other than PLXDC1 upregulation by the tumor cells, required restoration of the endothelial component of BBB, which would work as a scaffold for migration. In support of this finding, bevacizumab is known to restore the BBB function of U87MG brain xenografts and of human GBM as well.[55,56] To conclude, our work indicates that the brain infiltration induced by bevacizumab is mainly driven by the vascular endothelium. We suggest an additional interpretation of the infiltrative shift of GBM, whereby this antiangiogenic treatment elicits a vascular-like behavior of the tumor cells that depends on PLXDC1 activation and that requires the endothelial component of the BBB as a substrate (Fig. 6).

Acknowledgements

References

1. Stupp R, Hegi ME, Mason WP, et al. Effects of radiotherapy with concomitant and adjuvant temozolomide versus radiotherapy alone on survival in glioblastoma in a randomised phase III study: 5-year analysis of the EORTC-NCIC trial. *Lancet Oncol* 2009;10:459–66.
2. Semenza GL. HIF-1: using two hands to flip the angiogenic switch. *Cancer Metastasis Rev* 2000;19: 59–65.
3. Calabrese C, Poppleton H, Kocak M, et al. A perivascular niche for brain tumor stem cells. *Cancer Cell* 2007;11:69–82.
4. Gilbertson RJ, Rich JN. Making a tumour's bed: glioblastoma stem cells and the vascular niche. *Nature Rev Cancer* 2007;7:733–6.
5. Ricci-Vitiani L, Pallini R, Biffoni M, et al. Tumour vascularization via endothelial differentiation of glioblastoma stem-like cells. *Nature* 2010;468:824–8.
6. Chinot OL, Wick W, Mason W, et al. Bevacizumab plus radiotherapy-temozolomide for newly diagnosed glioblastoma. *N Engl J Med* 2014;370:709–22.
7. Taal W, Oosterkamp HM, Walenkamp AM, et al. Single agent bevacizumab or lomustine versus a combination of bevacizumab plus lomustine in patients with recurrent glioblastoma (BELOB trial): a randomised controlled phase 2 trial. *Lancet Oncol* 2014;15:943–53.

Molecular Cancer Biology

8. Wick W, Gorlia T, Bendszus M, et al. Lomustine and bevacizumab in progressive glioblastoma. N Engl J Med 2017;377:1954–63.

9. de Groot JF, Fuller G, Kumar AJ, et al. Tumor invasion after treatment of glioblastoma with bevacizumab: radiographic and pathologic correlation in humans and mice. Neuro Oncol 2010;12:233–42.

10. Gomez-Manzano C, Holash J, Fueyo J, et al. VEGF trap induces antiglioma effect at different stages of disease. Neuro Oncol 2008;10:940–5.

11. Pàez-Ribes M, Allen E, Hudock J, et al. Antiangiogenic therapy elicits malignant progression of tumors to increased local invasion and distant metastasis. Cancer Cell 2009;15:220–31.

12. Chamberlain MC. Radiographic patterns of relapse in glioblastoma. J Neurooncol 2011;101:319–23.

13. Huveldt D, Lewis-Tuffin LJ, Carlson BL, et al. Targeting Src family kinases inhibits bevacizumab-induced glioma cell invasion. PLoS One 2013;8:e56505.

14. Lucio-Eterovic AK, Piao Y, de Groot JF. Mediators of glioblastoma resistance and invasion during antivascular endothelial growth factor therapy. Clin Cancer Res 2009;15:4589–99.

15. Norden AD, Drappatz J, Wen PY. Novel anti-angiogenic therapies for malignant gliomas. Lancet Neurol 2008;7:1152–60.

16. Fischer I, Cunliffe CH, Bollo RJ, et al. High-grade glioma before and after treatment with radiation and Avastin: initial observations. Neuro Oncol 2008;10:700–8.

17. Rose SD, Aghi MK. Mechanisms of evasion to antiangiogenic therapy in glioblastoma. Clin Neurosurg 2010;57:123–8.

18. Lu KV, Bergers G. Mechanisms of evasive resistance to anti-VEGF therapy in glioblastoma. CNS Oncol 2013;2:49–65.

19. De Pascalis I, Morgante L, Pacioni S, et al. Endothelial trans-differentiation in glioblastoma recurring after radiotherapy. Mod Pathol 2018;31:1361–6. https://doi.org/10.1038/s41379-018-0046-2.

20. Moutal A, Honnorat J, Massoma P, et al. CRMP5 controls glioblastoma cell proliferation and survival through notch-dependent signaling. Cancer Res 2015;75:3519–28.

21. Tate CM, Blosser W, Wyss L, et al. LY2228820 dimesylate, a selective inhibitor of p38 mitogen-activated protein kinase, reduces angiogenic endothelial cord formation in vitro and in vivo. J Biol Chem 2013;288:6743–53.

22. Gentleman RC, Carey VJ, Bates DM, et al. Bioconductor: open software development for computational biology and bioinformatics. Genome Biol 2004;5:R80.

23. Ritchie ME, Phipson B, Wu D, et al. Limma powers differential expression analyses for RNA-sequencing and microarray studies. Nucleic Acids Res 2015;43:e47.

24. Subramanian A, Tamayo P, Mootha VK, et al. Gene set enrichment analysis: a knowledge-based approach for interpreting genome-wide expression profiles. Proc Natl Acad Sci USA 2005; 102:15545–50.

25. Martini M, de Pascalis I, D'Alessandris QG, et al. VEGF-121 plasma level as biomarker for response to anti-angiogenetic therapy in recurrent glioblastoma. BMC Cancer 2018;18:553.

26. Peterson TE, Kirkpatrick ND, Huang Y, et al. Dual inhibition of Ang-2 and VEGF receptors normalizes tumor vasculature and prolongs survival in glioblastoma by altering macrophages. Proc Natl Acad Sci USA 2016;113:4470–5.

27. Miller TE, Liau BB, Wallace LC, et al. Transcription elongation factors represent in vivo cancer dependencies in glioblastoma. Nature 2017;547:355–9.

28. Beaty RM, Edwards JB, Boon K, et al. PLXDC1 (TEM7) is identified in a genome-wide expression screen of glioblastoma endothelium. J Neurooncol 2007;81:241–8.

29. Carson-Walter EB, Hampton J, Shue E, et al. Plasmalemmal vesicle associated protein-1 is a novel marker implicated in brain tumor angiogenesis. Clin Cancer Res 2005;11:7643–50.

30. Mathiisen TM, Lehre KP, Danbolt NC, et al. The perivascular astroglial sheath provides a complete covering of the brain microvessels: an electron microscopic 3D reconstruction. Glia 2010;58:1094–103.

31. Granholm AC, Curtis M, Diamond DM, et al. Development of an intact blood-brain barrier in brain tissue transplants is dependent on the site of transplantation. Cell Transplant 1996;5:305–14.

32. Wick W, Chinot OL, Bendszus M, et al. Evaluation of pseudoprogression rates and tumor progression patterns in a phase III trial of bevacizumab plus radiotherapy/temozolomide for newly diagnosed glioblastoma. Neuro Oncol 2016;18:1434–41.

33. Nowosielski M, Ellingson BM, Chinot OL, et al. Radiologic progression of glioblastoma under therapy-an exploratory analysis of AVA-glio. Neuro Oncol 2018;20:557–66.

34. Kunkel P, Ulbricht U, Bohlen P, et al. Inhibition of glioma angiogenesis and growth in vivo by systemic treatment with a monoclonal antibody against vascular endothelial growth factor receptor-2. Cancer Res 2001;61:6624–8.

35. Otani Y, Ichikawa T, Kurozumi K, et al. Fibroblast growth factor 13 regulates glioma cell invasion and is important for bevacizumab-induced glioma invasion. Oncogene 2018;37:777–86.

36. Rubenstein JL, Kim J, Ozawa T, et al. Anti-VEGF antibody treatment of glioblastoma prolongs survival but results in increased vascular cooption. Neoplasia 2000;2:306–14.

37. Mesti T, Savarin P, Triba MN, et al. Metabolic impact of anti-angiogenic agents on U87 glioma cells. PLoS One 2014;9:e99198.

38. Ono T, Sasajima T, Doi Y, et al. Amino acid PET tracers are reliable markers of treatment responses to single-agent or combination therapies including temozolomide, interferon-beta, and/or bevacizumab for glioblastoma. Nucl Med Biol 2015;42:598–607.

39. Grossman R, Brastianos H, Blakeley JO, et al. Combination of anti-VEGF therapy and temozolomide in two experimental human glioma models. J Neurooncol 2014;116:59–65.

40. Saidi A, Hagedorn M, Allain N, et al. Combined targeting of interleukin-6 and vascular endothelial growth factor potently inhibits glioma growth and invasiveness. Int J Cancer 2009;125:1054–64.

41. de Groot J, Milano V. Improving the prognosis for patients with glioblastoma: the rationale for targeting Src. J Neurooncol 2009;95:151–63.

42. Tsai HH, Niu J, Munji R, et al. Oligodendrocyte precursors migrate along vasculature in the developing nervous system. Science 2016;351:379–84.

43. Griveau A, Seano G, Shelton SJ, et al. A glial signature and Wnt7 signaling regulate glioma-vascular interactions and tumor microenvironment. Cancer Cell 2018;33:874–89.

44. Piao Y, Liang J, Holmes LS, et al. Acquired resistance to anti-VEGF therapy in glioblastoma is associated with a mesenchymal transition. Clin Cancer Res 2013;19:4392–403.

45. Urup T, Staunstrup LM, Michaelsen SR, et al. Transcriptional changes induced by bevacizumab combination therapy in responding and non-responding recurrent glioblastoma patients. BMC Cancer 2017;17:278.

46. Iwamoto FM, Abrey LE, Beal K, et al. Patterns of relapse and prognosis after bevacizumab failure in recurrent glioblastoma. Neurology 2009;73:1200–6.

47. Delay M, Jahangiri A, Carbonell WS, et al. Microarray analysis verifies two distinct phenotypes of glioblastomas resistant to antiangiogenic therapy. Clin Cancer Res 2012;18:2930–42.

48. Ricci-Vitiani L, Pallini R, Larocca LM, et al. Mesenchymal differentiation of glioblastoma stem cells. Cell Death Differ 2008;15:1491–8.

49. Wang R, Chadalavada K, Wilshire J, et al. Glioblastoma stem-like cells give rise to tumour endothelium. Nature 2010;468:829–33.

50. Miller SF, Summerhurst K, Rünker AE, et al. Expression of Plxdc2/TEM7R in the developing nervous system of the mouse. Gene Expr Patterns 2007;7:635–44.

51. Lee HK, Seo IA, Park HK, et al. Identification of the basement membrane protein nidogen as a candidate ligand for tumor endothelial marker 7 in vitro and in vivo. FEBS Lett 2006;580:2253–7.

52. Nanda A, Buckhaults P, Seaman S, et al. Identification of a binding partner for the endothelial cell surface proteins TEM7 and Tem7r. cancer Res 2004;64:8507–11.

53. Zhang ZZ, Hua R, Zhang JF, et al. TEM7 (PLXDC1), a key prognostic predictor for resectable gastric cancer, promotes cancer cell migration and invasion. Am J Cancer Res 2015; 5:772–81.

54. Bagley RG, Rouleau C, Weber W, et al. Tumor endothelial marker 7 (TEM-7): a novel target for antiangiogenic therapy. Microvasc Res 2011;82:253–62.

55. Okamoto S, Nitta M, Maruyama T, et al. Bevacizumab changes vascular structure and modulates the expression of angiogenic factors in recurrent malignant gliomas. Brain Tumor Pathol 2016;33:129–36.

56. Stegmayr C, Oliveira D, Niemietz N, et al. Influence of bevacizumab on blood-brain barrier permeability and O-(2-18F-Fluoroethyl)-l-tyrosine uptake in rat gliomas. J Nucl Med 2017;58:700–5.